JOURNAL OF MATERIALS SCIENCE **34** (1999) 4737–4749

Structure-property relations for silicon nitride matrix composites reinforced with pyrolytic carbon pre-coated Hi-Nicalon fibers

B. J. KOOI, J. Th. M. DE HOSSON
Department of Applied Physics, Materials Science Centre, University of Groningen, Nijenborgh 4, 9747 AG Groningen, The Netherlands
E-mail: B.J.Kooi@phys.rug.nl; hossonj@phys.rug.nl

C. OLIVIER*, J. B. VEYRET
Institute for Advanced Materials, Joint Research Centre, P.O. Box 2, 1755 ZG Petten, The Netherlands

Si_3N_4 matrix composites reinforced with pyrolytic carbon pre-coated Hi-Nicalon (SiC) fibers, were studied using tensile testing and transmission electron microscopy. Three types of samples were evaluated all with a nominal coating thickness of 200 nm. The composites were densified by hot pressing at 1550 °C (type I and II) and at 1600 °C (type III). The fibers were coated with pyrolytic carbon via CVD with identical (sample I) and opposite (samples II and III) directions of the gas flow and of the fiber movement through the reactor. Tensile testing indicated for the three sample types respectively: brittle behaviour with huge pull out of the fibers, pseudo-plastic behaviour and brittle behaviour with little pull out. TEM indicated for the three sample types debonding typically at the fiber/coating interface, at the coating/matrix interface and in the coating, respectively. The relation between processing, structure, particularly of the coating and its interfaces with the matrix and the fibers and mechanical properties is addressed.

1. Introduction

Ceramic materials offer excellent temperature, corrosion and wear resistance, but their wide application is severely limited by their brittleness and low fracture toughness. These limitations can be overcome by fiber reinforcement. However, in order to improve the fracture toughness without too much degrading the other performances, the intrinsic properties of the fiber material should be comparable with the ones of the matrix.

Si_3N_4 is interesting owing to its low density, high strength and refractoriness. Long carbon fiber reinforcement can improve the toughness [1], but, although the thermal resistance of the carbon fibers is sufficient to withstand temperatures of 1600 °C, e.g. as used for sintering Si_3N_4, oxidation of the fibers already poses problems above 500 °C. Also so-called Nicalon (SiC) fibers (Nippon Carbon), containing up to 12 wt % oxygen resulting in meta-stable silicon oxycarbide, exhibit insufficient thermal stability mainly due to decomposition of the oxycarbide [2, 3]. For the subsequently developed Hi-Nicalon (SiC) fibers this stability has been greatly improved by a reduction of the oxygen content to below 0.5 wt % [4]. Consequently, Hi-Nicalon fiber reinforcement is promising for high temperature applications and can also endure the high temperatures employed during densification of the Si_3N_4 composites [5].

Hi-Nicalon fiber reinforced Si_3N_4 matrix composites exhibit brittle fracture if the matrix is directly sintered to the fibers [5, 6]. After tensile testing of unidirectionally oriented fiber composites with loading in a direction parallel to the fiber axes, the fracture surface showed no pull out of the fibers. Apparently, a strong fiber/matrix bond is achieved. An interphase between the fiber and the matrix is needed in order to decrease the strength of this bond. Pre-coating the fibers with pyrolytic carbon (C_P) was shown to be effective in causing improved toughness of the subsequently obtained composites [5, 6].

In the present study the fibers were coated with 200 nm thick C_P and differences between samples were invoked by two hot-pressing temperatures (1550 and 1600 °C) used for densification of the composites and by two different CVD process conditions during coating deposition. The composites were studied by room temperature tensile testing and by high-resolution transmission electron microscopy (HRTEM) with the aim to correlate the structure and the mechanical properties. Since the C_P coating plays a crucial role with respect to the mechanical performance of the composites the

* *Present address*: TWI, Abington Hall, Abington Cambridge CB1 6AL, UK.

TEM study has concentrated on the coating and on its interfaces with the fiber and the matrix.

2. Experimental

2.1. Manufacturing of Hi-Nicalon fiber reinforced Si_3N_4

The composite fabrication methodology was adapted from the one developed earlier at IAM Petten for carbon-fiber reinforced Si_3N_4 materials [7]. Unidirectional fiber preforms infiltrated with a dispersion of submicron silicon nitride powder and 10 wt % of sintering additives (Al_2O_3, Y_2O_3) in de-ionized water were densified by hotpressing under 27 MPa pressure to ca. 98% theoretical density with 35 vol % fiber. In order to decrease the interfacial bond strength and to avoid the brittle fracture of the composites, a pyrolytic carbon coating was deposited on the Hi-Nicalon fibres, prior to fabrication, using a low pressure chemical vapour deposition technique [8, 9] (performed at the "Laboratoire des Multimatériaux et Interfaces", Université Claude Bernard-Lyon, France). During deposition of the C_P coating the fibers are transported with a chosen constant speed through the CVD reactor using supply/take-up reels on both ends of the reactor, where the whole set-up is placed in a stainless steel vacuum chamber [9]. In the present study three different types of samples are addressed all with a nominal coating thickness of 200 nm. Sample types I and II were densified by hot-pressing at 1550 °C, whereas sample type III was hot-pressed at 1600 °C. The difference between sample I and II/III is a result of changing the fiber-transport direction with respect to the gas-flow direction through the CVD reactor during the deposition of the C_P coating. For sample type I both directions were the same, whereas for sample types II and III both directions were opposite.

2.2. Tensile testing

Tensile testing of the composites was performed, at room temperature, on a servo-hydraulic Instron testing machine 8511. The specimens ($72 \times 7 \times 1.2$ mm^3) were loaded in a direction parallel to the fiber axis. Monotonic tensile tests were achieved with a constant cross-head speed of 0.05 mm/min. Aluminum tabs were glued with epoxy on the specimen ends to provide an uniform gripping pressure and to avoid damage from the grip surfaces. Strain was measured using a 14 mm gauge length Schenk extensometer clamped on the thinner surface of the specimen.

2.3. TEM analysis

TEM samples were prepared by grinding, dimpling and ion milling (4 kV Ar ions under 13°) 3 mm discs to electron transparency. The discs were cut perpendicular to the fiber axes, i.e. with the fiber axes in the plane of the discs. For TEM, a JEOL 4000 EX/II, operating at 400 kV (spherical aberration coefficient: 0.97 ± 0.02 mm, defocus spread: 7.8 ± 1.4 nm, beam semi-convergence angle: 0.8 mrad) with a point resolution of 0.17 nm, was used.

3. Results

3.1. Tensile testing

Typical stress-strain curves of the three types of samples (see Section 2.1) are shown in Fig. 1.

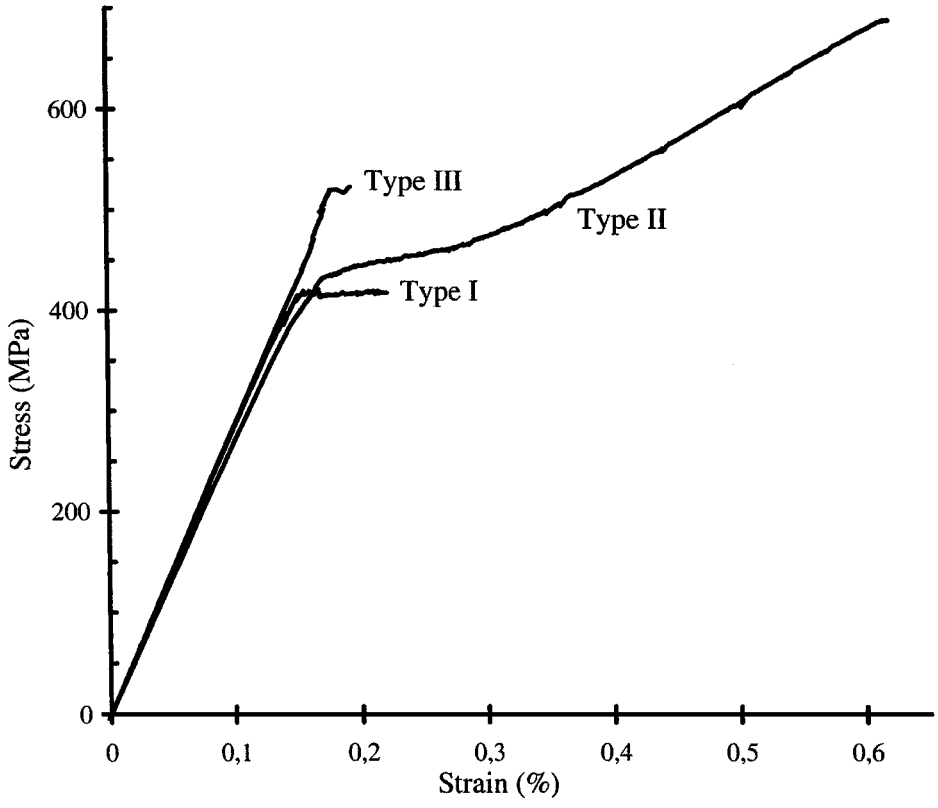

Figure 1 Stress-strain curves of three different types of unidirectionally Hi-Nicalon fiber reinforced Si_3N_4 matrix composites (see text). The loading during tensile testing was in a direction parallel to the fiber axis.

3.1.1. Type I

Type I composites exhibit an initial elastic behaviour up to a stress of 390 ± 20 MPa. When the applied stress exceeds the elastic limit, the matrix micro-cracks, resulting in a rapid increase in strain. However, failure i.e. overall fracture of the composite already occurs during the matrix micro-cracking stage for a stress of 430 ± 50 MPa. The fracture surfaces exhibit a huge pull-out of the broken fibers ranging from 500 to 1000 μm. These results suggest a very low frictional stress at the fiber-matrix interface thus reducing the efficiency of the stress transfer mechanism after matrix cracking. As a consequence, the bridging fibers are greatly overloaded and this overload occurs on long distances on both sides of each matrix crack leading to failure of the material before the matrix cracking saturates.

3.1.2. Type II

Type II composites exhibit three stages of composite fracture: an initial elastic region up to about 390 ± 40 MPa followed by a period of progressive matrix micro-cracking with interface debonding and load transfer to the fibers and finally, after saturation of matrix cracking, an elastic region where the applied load is mainly sustained by the surviving fibers until 700 ± 50 MPa. Fracture occurs with an extensive and regular fiber pull-out of 200 μm average length.

3.1.3. Type III

Type III composites exhibit an initial elastic region up to a stress of 410 ± 20 MPa followed by matrix micro-cracking. The higher elastic limit obtained for composites III compared to composites II is a direct consequence of the increase of the matrix strength upon hot-pressing at a higher temperature (1600 instead of 1550 °C) [10]. However, matrix-cracking initiation is soon followed by the fracture of the composites for a stress of 430 ± 20 MPa. Observations of the fracture surfaces exhibited a nonregular and short fiber pull-out of 30 μm average length. These results suggest that the decohesion at the interface was partly initiated but the interfacial bonding was still high enough to promote fiber fracture in close proximity to the crack front resulting in low toughness.

3.2. TEM analysis

3.2.1. Type I

Debonding of the C_P coating from both the SiC fiber and the Si_3N_4 matrix can be observed in the bright field image of sample type I shown in Fig. 2. Such a debonding between the coating and the fiber was never observed in the types II and III. Due to the TEM sample preparation the gap between the fiber and the matrix may have been enlarged or stress relaxation after this preparation may even has caused this debonding, but still the conclusion holds, from comparison with the images obtained for the samples II and III (see below), that the coating is not well-bonded to the matrix and, particularly, the bonding to the fiber is very poor.

The weakness of the bonding between the coating and the fiber becomes obvious in Fig. 3, where the coating is debonded from the fiber, but on the other hand is still attached to the Si_3N_4. Fiber/coating debonding appeared typical for sample I. Due to porosity at the matrix/coating interface, the coating is bonded to the matrix at relative small portions of the observed interface length. The sample is relatively thick for TEM in the area shown in Fig. 3, but this is on purpose, because it diminishes the possible influence of the TEM sample preparation on the observed microstructure. The coating, with nominal thickness of 200 nm, does not appear uniform: a layer of about 120 nm at the fiber side is distinct from a layer of about 160 nm at the matrix side. The 120 nm part of the coating is darker and shows smaller intensity variations than the 160 nm part. This two-sublayers structure of the coating was observed often in sample I. Finally, some porosity in the Si_3N_4 matrix can be observed in Fig. 3.

In the cases where the coating is still attached to the SiC fiber areas of weakness, where elongated "holes" along the coating/fiber interface are present, were observed often; see Fig. 4a. Instead of holes it could also be small areas where the mass-thickness is significantly smaller than in the surrounding material. Also this feature of "holes" is typical for sample I and was not observed in the other two types of samples. In the C_P coating shown in Fig. 4a, a change in structure of the coating as a function of distance to the coating/fiber interface can be observed. Near to the fiber a fine "granular" structure is present, which coarsens dramatically with increasing distance to the interface. This coarsening can be associated with an increasing size of densely packed bundles of parallel oriented {001} planes in the C_P.

Observation at the atomic level of the interface between the C_P coating and the SiC fiber may give clues for their poor bonding and therefore HRTEM imaging of these interfaces was performed. The weakest parts of the interface where debonding has occurred are the most interesting ones. However, it is impossible to observe the original coating and fiber sides that were formerly joined at the interface, because these sides are certainly damaged by ion milling. Only at the less interesting parts, where the coating is still attached to the fiber and thus being less representative for the weak bonding, the interface structure can be examined.

A HRTEM image of a region containing a "hole" as could be observed in Fig. 4a is shown in Fig. 4b. In this case, as in most other cases, it did not appear a real hole, but only an area that to a larger extent approaches a weak-phase object than its surrounding. So, in these areas the product of density and thickness is significantly less and/or the structure is more random/amorphous than in the surrounding areas. Still, similar fringes as in the C_P could be observed in these areas (more clearly at other defocus values than for the image shown) indicating that they contain very thin C_P. On the fiber side directly adjacent to this minimum-contrast C_P area in Fig. 4b, a layer with a width of 5 to 10 nm is present with a structure which differs from the one of the

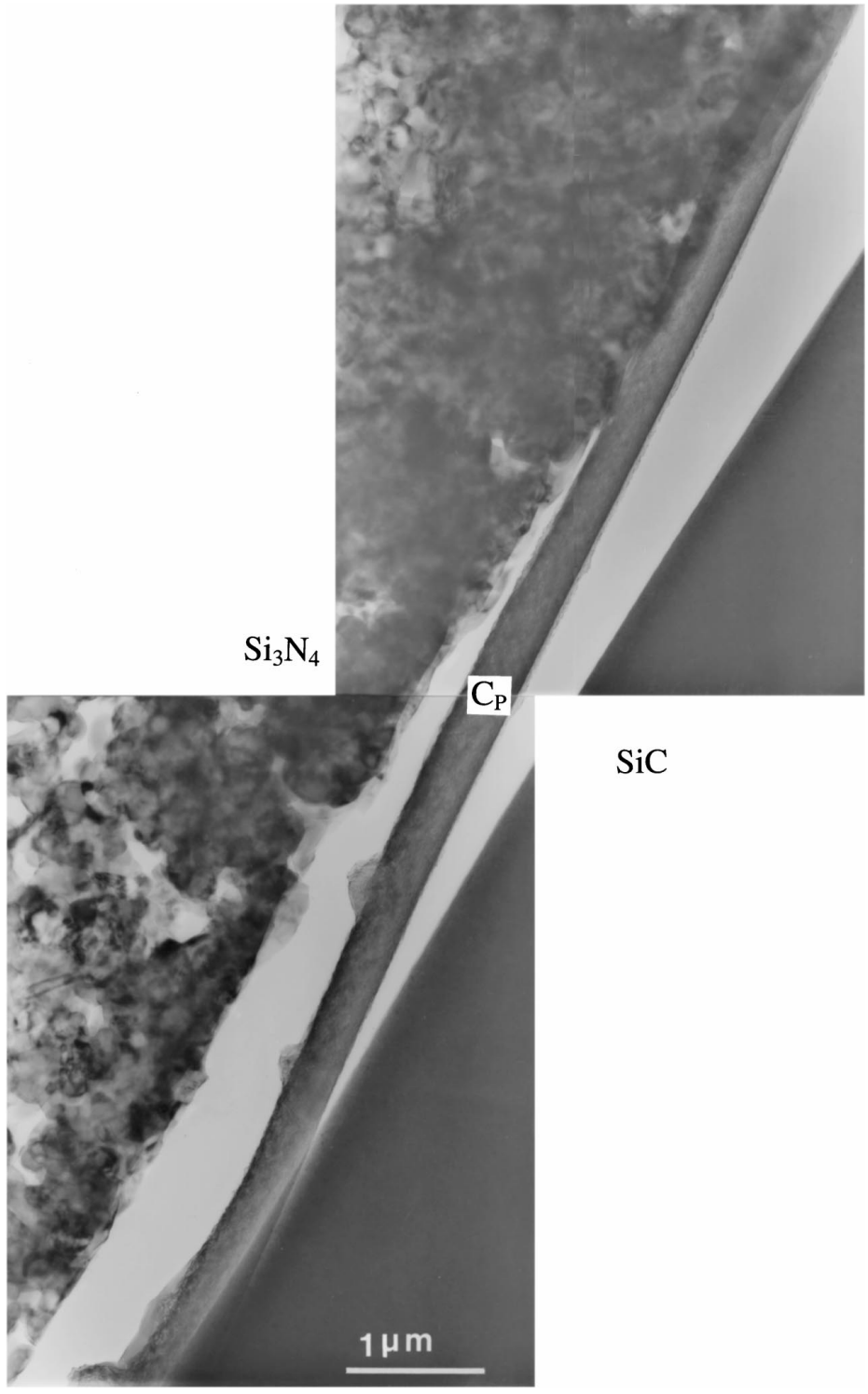

Figure 2 Pyrolytic carbon (C_P) coating is debonded from both the Hi-Nicalon (SiC) fiber and the Si_3N_4 matrix in sample type I.

nanocrystalline SiC and from the parallel-fringed C_P. Although giving more contrast than the neighbouring C_P, which is a consequence of a larger mass-thickness, the structure is more amorphous-like than either the C_P or the SiC. As a possible candidate for this unknown structure at the C_P/SiC interface, amorphous SiO_2 is an obvious choice. SiO_2 is a more stable phase than (all polymorphs of) SiC and may also be present as a native oxide film on the SiC fibers. The "holes" in the C_P adjacent to the SiO_2 now gives the impression that SiO_2 on the fiber surface leads to a reduced "wetting" by C_P. Apparently the C_P prefers to be bonded to SiC instead of SiO_2. This is in agreement with observations that the presence of SiO_2 instead of SiC at the fiber surface diminishes the bond strength between the fiber and the C_P coating [3]. Further, the type of elongated "holes" that can be observed in Fig. 4a shows remarkable resemblance, although somewhat less extreme, with the debonding cracks at the Nicalon-fiber/C_P-coating interface shown in Ref. [11] that were a consequence of 1300 °C oxidation in air of a Nicalon fiber reinforced SiC matrix composite. Already during the deposition of the coating the "holes" could have formed, but their formation during sintering is also very well possible. A

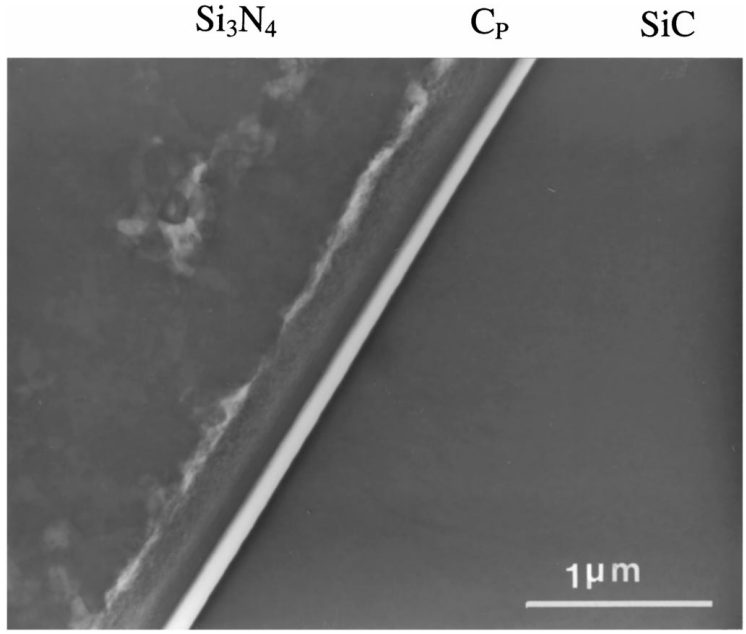

Figure 3 Pyrolytic carbon (C_P) coating is debonded from the Hi-Nicalon fiber, but still attached to the Si_3N_4 matrix in sample type I. A relative large amount of porosity is present at the coating/matrix interface. A thick part of the TEM sample is shown in order to diminish the possible influence of the TEM sample preparation.

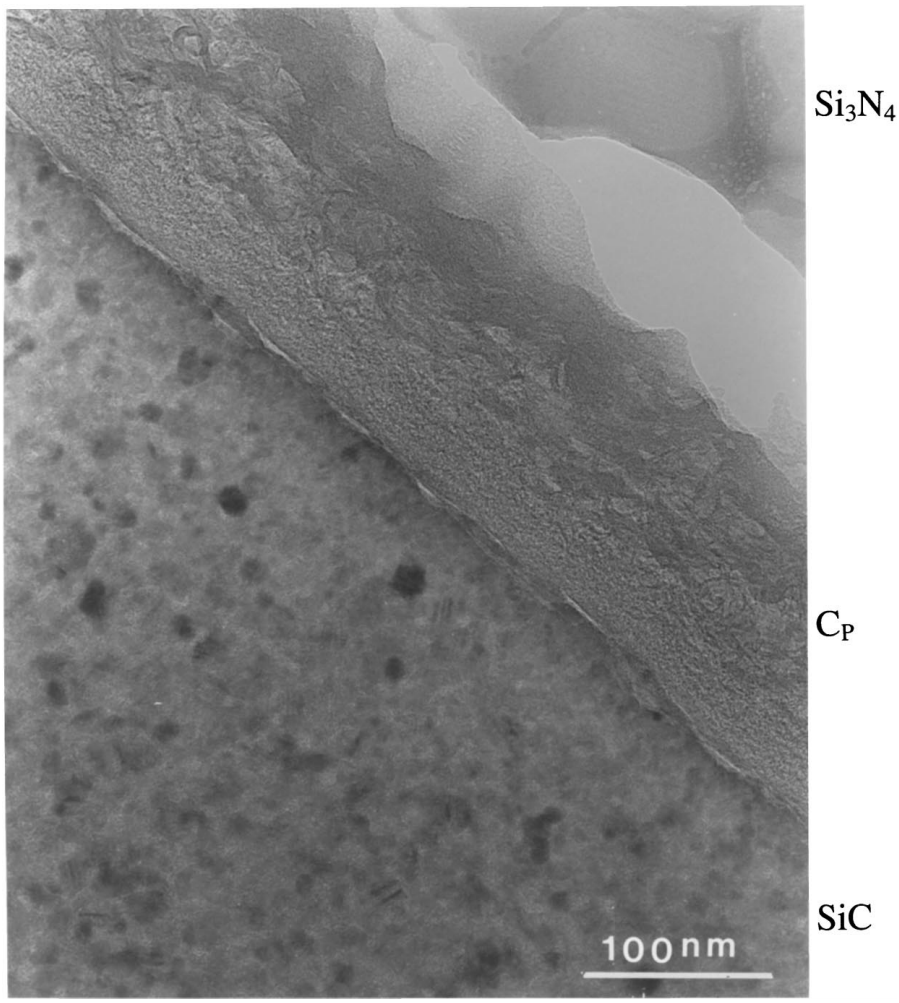

(a)

Figure 4 (a) When the pyrolytic carbon (C_P) coating is still attached to the Hi-Nicalon (SiC) fiber in sample type I, elongated holes at the fiber/coating interface can be observed. The micro-structure of the coating exhibits a gradual change as a function of distance to the fiber/coating interface (compare with Fig. 6) and (b) HRTEM image showing in detail a region with an elongated hole at the fiber/coating interface. In fact it is not really a hole, but an area in the pyrolytic carbon (C_P) with a much smaller mass-thickness than its surrounding. At the fiber side of this area amorphous SiO_2 is present instead of SiC. The impression is obtained that the presence of SiO_2 is responsible for the occurrence of the "holes" at the coating/fiber interface and for the poor bonding between fiber and coating. (*Continued*).

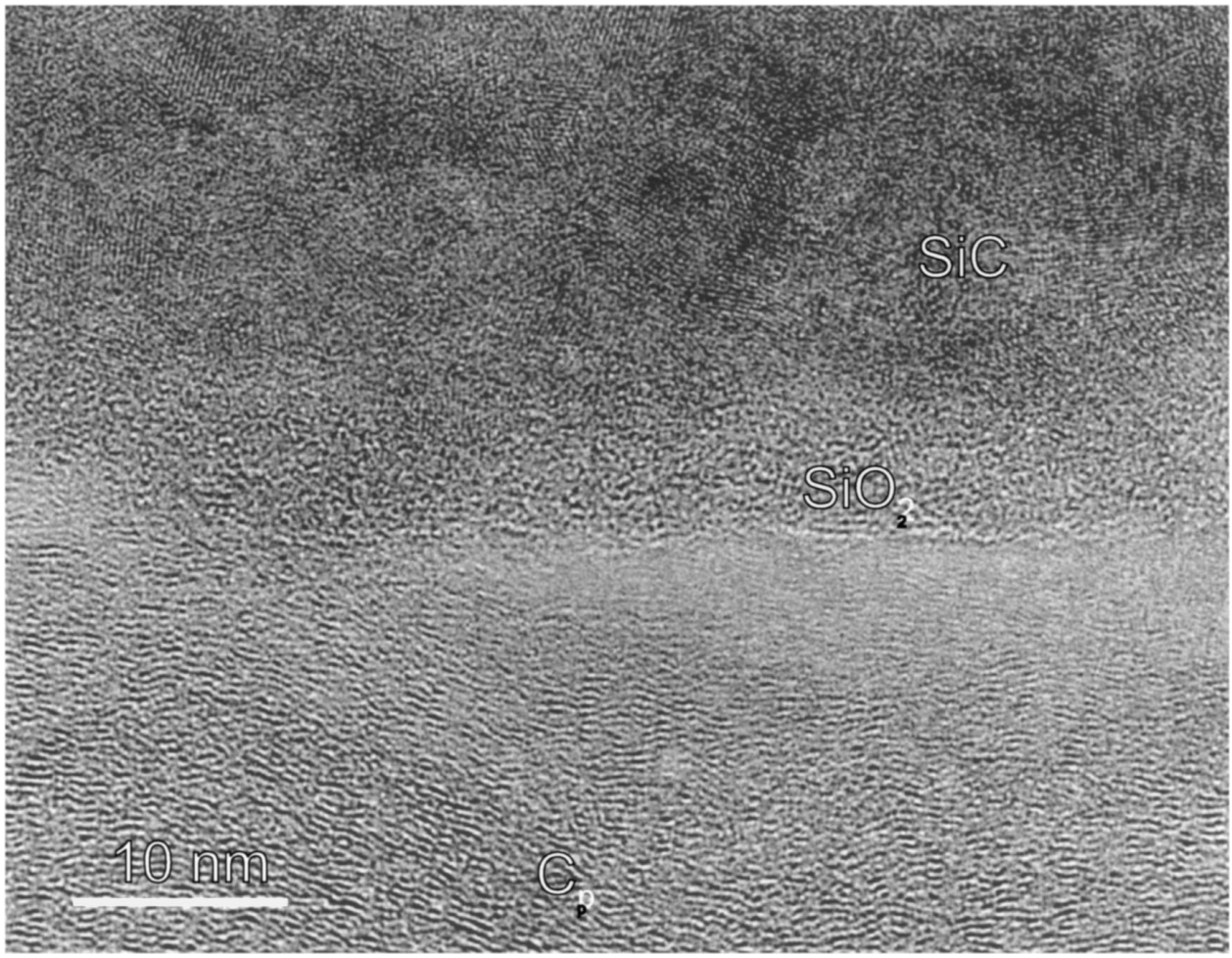

(b)

Figure 4 (*Continued*).

reaction of SiO_2 with the C_P to form SiC and gaseous CO is, using the bulk phase thermodynamic data of Ref. [12], just possible (negative change in Gibbs-free energy) at the sintering temperature 1550 °C, whereas this reaction is not feasible at the lower temperature used for coating deposition.

Apart from the "holes", another clearly observable difference between the coating/fiber interface in sample type I and this interface in the other two types of samples (which will be shown below) is the smoothness of the interface where the {001} type planes in the C_P are all aligned relatively parallel to each other, to the interface and to the fiber axis. This high degree of parallelism was not observed in the other two types of samples.

3.2.2. Type II

TEM images of the interface region where the SiC fiber and the Si_3N_4 matrix are bonded via the C_P coating are presented in Figs 5–8 for sample II. The C_P coating appeared to have a very non-uniform thickness; Figs 5 and 7. With respect to the scale shown, the fiber/coating interface is very straight compared to the coating/matrix interface. At some interfaces a coating between the SiC and the Si_3N_4 could not be detected and at most interfaces the coating was smaller than the expected nominal

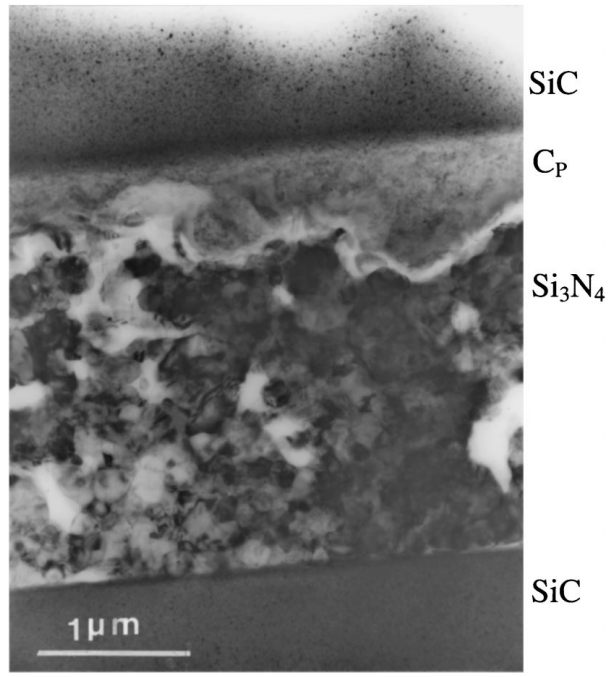

Figure 5 The C_P coating of sample type II exhibits a very non-uniform thickness. At some interfaces a coating between the SiC fiber and the Si_3N_4 matrix can not be detected and at most interfaces the coating is smaller than the expected nominal thickness of 200 nm, but then at some parts the coating is much thicker than 200 nm.

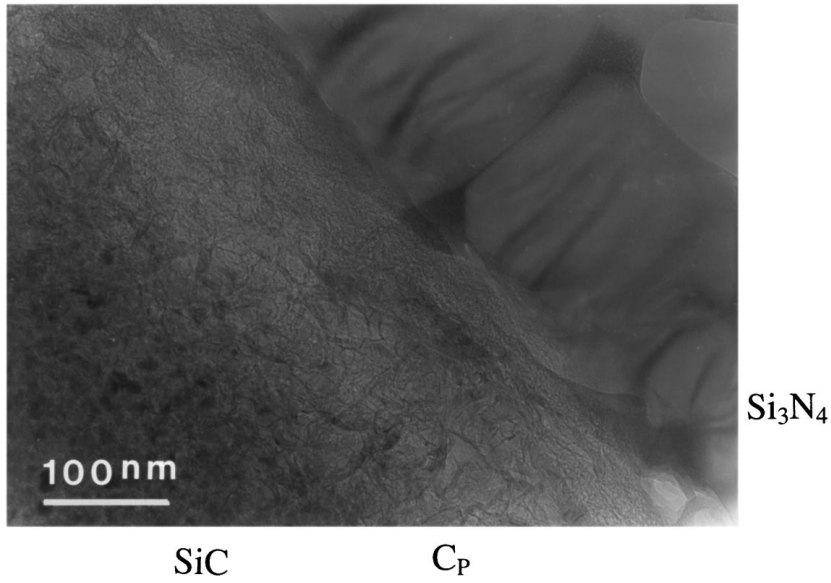

Figure 6 Pyrolytic carbon (C_P) coating is (after tensile testing still) well bonded to both the Hi-Nicalon fiber and the Si_3N_4 matrix in sample type II. The micro-structure of the coating exhibits a gradual change as a function of distance to the fiber/coating interface, which is reversed with respect to the micro-structural evolution exhibited by the coating shown in Fig. 4a.

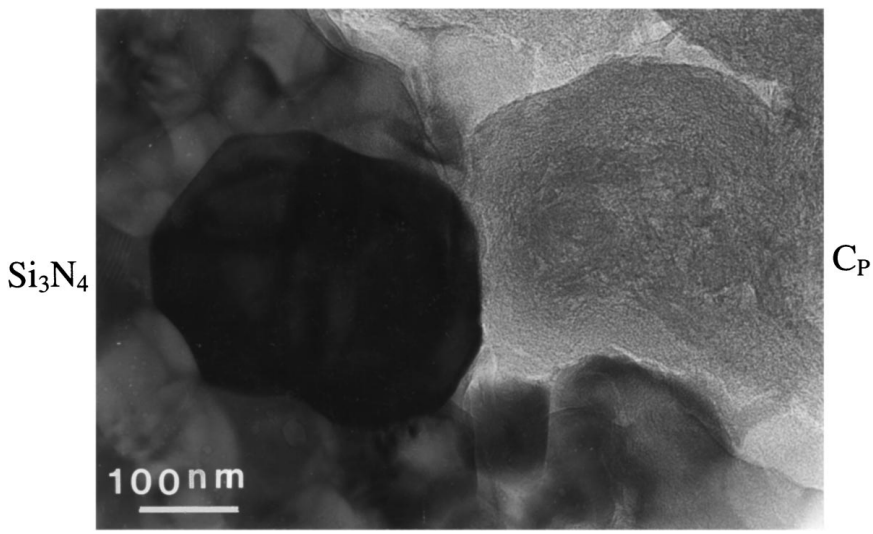

Figure 7 The pyrolytic carbon (C_P) shown, gives the impression to be rolled into a ball between the Si_3N_4 matrix and the fiber. This impression holds for the total coating adjacent to the small part shown. Possibly, this rolling is a result of the sliding between the fiber and the matrix for a rough coating/matrix interface during tensile testing.

thickness of 200 nm, but then at some parts the coating was much thicker than 200 nm; Fig. 5. Also at relatively large distances from the coating, pyrolytic carbon could be detected in-between the Si_3N_4 grains. Porosity was observed in the Si_3N_4 matrix and particularly at the matrix/coating interface.

Debonding between the Si_3N_4 matrix and the C_P coating was observed in a number of cases (and could have occurred as a consequence of TEM sample preparation), whereas debonding between the coating and the SiC fiber was never observed.

In the C_P coating shown in Fig. 6 a change in microstructure of the coating as a function of distance to the coating/fiber interface can be observed which is the reverse of the micro-structural evolution exhibited by the coating in Fig. 4a. A fine "granular" structure is now present near the matrix instead of near the fiber (can also be seen in Fig. 7). The structure coarsens dramatically with increasing distance to the matrix/coating instead of to the fiber/coating interface. Near the fiber, the orientation of the planes in the pyrolytic carbon is "wild" (Figs 6 and 8). In small bundles the planes are aligned parallel, but these bundles can be extremely curved and non-parallel with each other, having a random and turbulent distribution giving the appearance of a stirred liquid. A sharp distinct interface, as was seen in sample I, with the {001}C_P planes all parallel to the fiber axis is absent in sample II.

The C_P shown in Fig. 7, being typical for the whole C_P coating of the adjacent fiber, gives the impression to be rolled into a ball between the matrix and the fiber. This may have occurred during manufacturing of the composite, but since Fig. 7 is obtained for a sample which was first tensile tested before TEM examination,

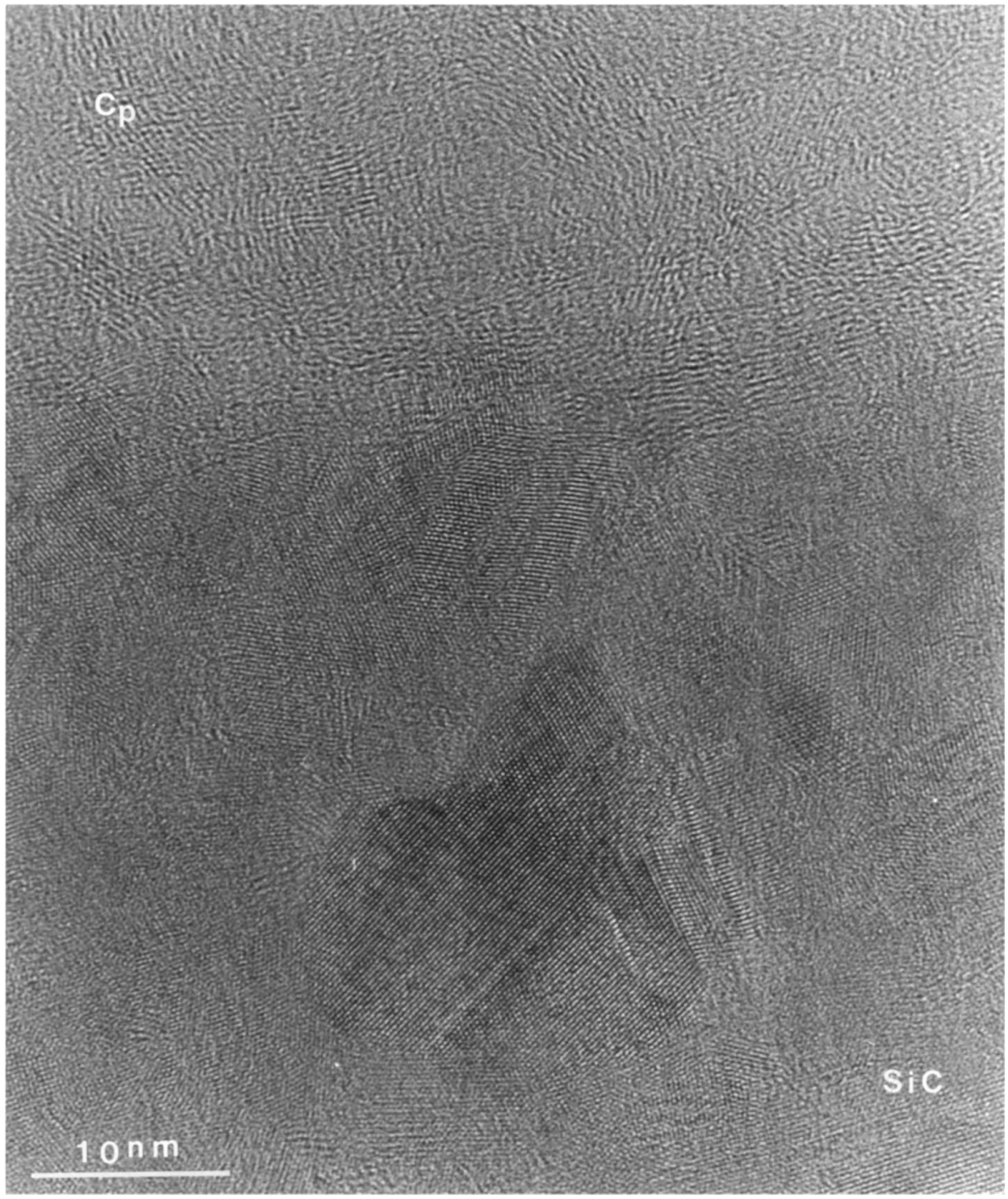

Figure 8 HRTEM image showing in detail the interface between the pyrolytic carbon and the Hi-Nicalon (SiC) fiber. The orientation of the {001} planes in the C_P in sample type II is wild and not parallel to the fiber axis as is the case for sample type I (cf. Fig. 4b).

this rolling may be a result of the sliding between the fiber and the matrix for a rough coating/matrix interface.

3.2.3. Type III

TEM images of sample III are presented in Figs 9–11. The C_P coating appears to be well-bonded to both the SiC fiber and the Si_3N_4 matrix; Figs 9 and 10a. A good bonding between the coating and the fiber was also observed for sample II, but now particularly the bonding of the coating to the matrix appears to be rather strong. This can deduced from Figs 9 and 10a, where "cracks" in the pyrolytic carbon coating occur instead of at the interface between the coating and the matrix (or at the interface with the fiber) and from Fig. 10b where the bonding of the coating to the matrix is so strong that grains of the Si_3N_4 are pulled out of the matrix. The images shown for type III are of a sample which was tensile tested before TEM analysis and the cracks in the coating and the pulling out of the Si_3N_4 grains are a consequence of this tensile testing. In this sample also cracks in the SiC fiber were observed, which were more or less an undeflected continuation of cracks in the matrix.

In sample I and II porosity in the Si_3N_4 matrix and particularly at the matrix/coating interface was observed. In sample III porosity in the matrix and at the matrix/coating interface was hardly detectable, resulting in a stronger bond between matrix and coating in sample III than in the other two types of samples.

At several locations the coating between the matrix and the fiber appeared to be absent and direct bonding between the Si_3N_4 and the SiC was achieved. An example of this phenomenon is given in Fig. 11. Fig. 11a shows a bright-field image and Fig. 11b shows an enlarged part of this image using HRTEM (phase contrast instead of diffraction contrast).

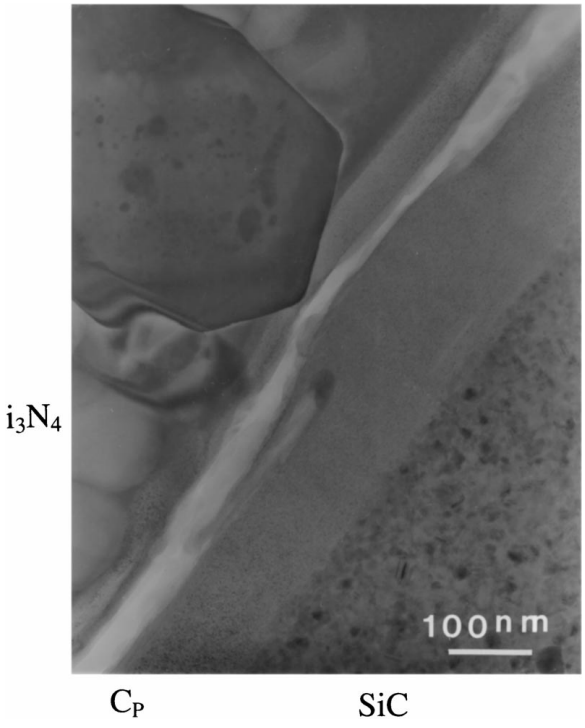

Figure 9 After tensile testing, sample type III exhibits cracks in the pyrolytic-carbon (C_P) coating and not debonding between the coating and the SiC fiber or the Si_3N_4 matrix.

4. Discussion

Differences between sample I and II are a consequence of a difference in deposition conditions of the C_P coating on the SiC fiber; for sample I the gas flow during CVD was in the same direction as of the pulling of the fibers through the reactor, whereas in sample II these two directions were opposite. Differences between sample II and III are caused by a difference in hot-pressing temperature during the densification of the CMC; sample II is hot pressed at 1550 °C, whereas sample III is hot pressed at 1600 °C. Differences between sample I and III can not be interpreted directly since both the condition of deposition of the coating and the hot-pressing temperature have been changed. Samples I and II and samples II and III are compared in Sections 4.1 and 4.2 respectively.

4.1. Influence of process conditions during CVD of pyrolytic carbon on SiC fiber

The weakness of sample I compared to sample II, i.e. brittle versus pseudo-plastic behaviour, as was directly determined by tensile testing is also easily recognizable in the TEM images. The huge pull-out of the fibers from the matrix during the tensile test indicated an insufficient load transfer from the matrix to the fiber in the case of sample I. The material behaves similar as monolithic Si_3N_4. From the TEM images it becomes apparent that the interface between the C_P coating and the SiC fiber is the weakest link. This is of course also noticeable from the tensile test by observing fibers which have lost their coating during pull-out. In sample II the coating/matrix interface appears the weakest point and in sample III the pyrolytic carbon coating itself instead of its interface with the matrix or the fiber is observed weakest.

Comparing samples I and II it is clear that the weakness of sample I is related to the CVD process in which the coating is deposited onto the fiber. Apparently the direction of the gas flow with respect to the pulling direction of the fibers through the reactor during the CVD process has significant influence on the bonding of the coating to the fiber. If the CVD conditions at both ends of the reactor were identical no difference between sample I and II would have been occurred.

Obviously, this is not the case and this was already shown in Ref. [8, 9] for static fibers (i.e. not pulled through the reactor) where clear morphological differences were observed between the coating deposited at the side where the gas entered and at the side where the gas left the reactor. At the gas entrance the coating appeared smooth with the {001} of the C_P mainly parallel to the fiber surface and this changed gradually to a coating surface which appeared to have blisters (not hollow) and finally to a very rough, open and porous, i.e. cauliflower-like surface resulting from a dendritic-like growth. The occurrence of these morphological chances was ascribed to the evolution of the concentration of the gaseous species as a function of position in the reactor [8, 9].

In the case the fiber is not static but pulled through the reactor, the micro-structure of the coating becomes at all lateral positions on the fiber the same. However, now an evolution of the micro-structure as a function of coating thickness, i.e. radial position occurs instead. Subsequently, it is readily understood that a reversal in direction of gas flow with respect to of the movement of the fiber will reverse this evolution of the micro-structure as a function of the radial position. For sample I the deposition started at the gas entrance, whereas for sample II it started at the gas exit. On the basis of the morphological results for deposition on the static fiber, the expected structure of the C_P at the fiber surface for sample I is smooth with the C_P{001} all parallel to the fiber surface and for sample II is much less ordered. This is exactly what is observed according to the TEM results presented in this paper. The reversal in evolution of the microstructure of the C_P coating can also be directly observed by comparing Figs 4a and 6.

However, the consistence between micro-structural change as a function of lateral position in the reactor in the case of a static fiber and as a function of the radial position in the coating in the case of pulled fibers does not explain the difference in the strength with which the C_P is bonded to the Hi-Nicalon fiber. The observation of the "holes" in the C_P adjacent to SiO_2 at the coating/fiber interface in the case of sample type I and the absence of these "holes" in the other two types of samples indicate that the presence of SiO_2 at the fiber surface is probably responsible for the deterioration of the coating/fiber bond.

Two reasons for the presence of SiO_2 at the fiber surface of sample type I and its absence on the other two types of samples can be put forward:

(i) SiO_2 is already present as a native oxide on the Hi-Nicalon fibers when they are introduced in the CVD

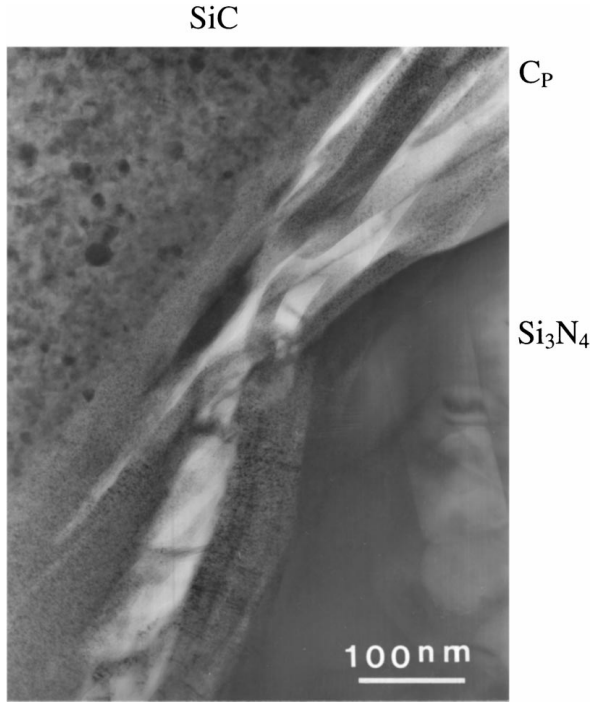

(a)

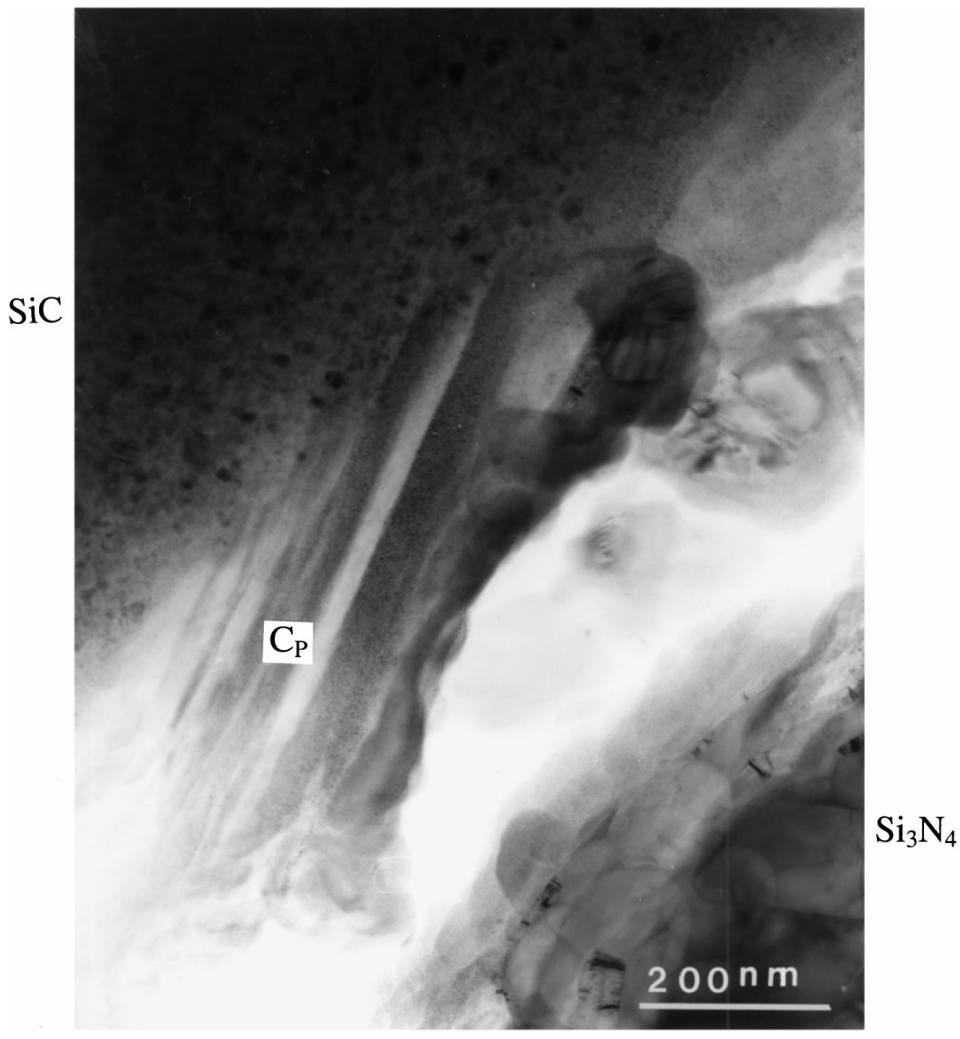

(b)

Figure 10 (a) After tensile testing, the pyrolytic carbon (C_P) coating in sample type III is highly stretched, resulting in many cracks and (b) The bonding between the C_P and both the Hi-Nicalon fiber and the Si_3N_4 matrix is that strong in sample type III that during tensile testing Si_3N_4 grains are pulled out of the matrix.

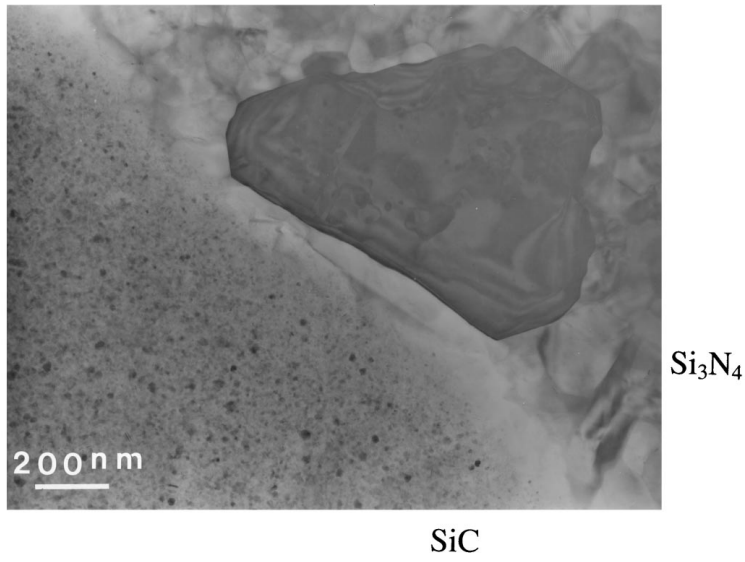

(a)

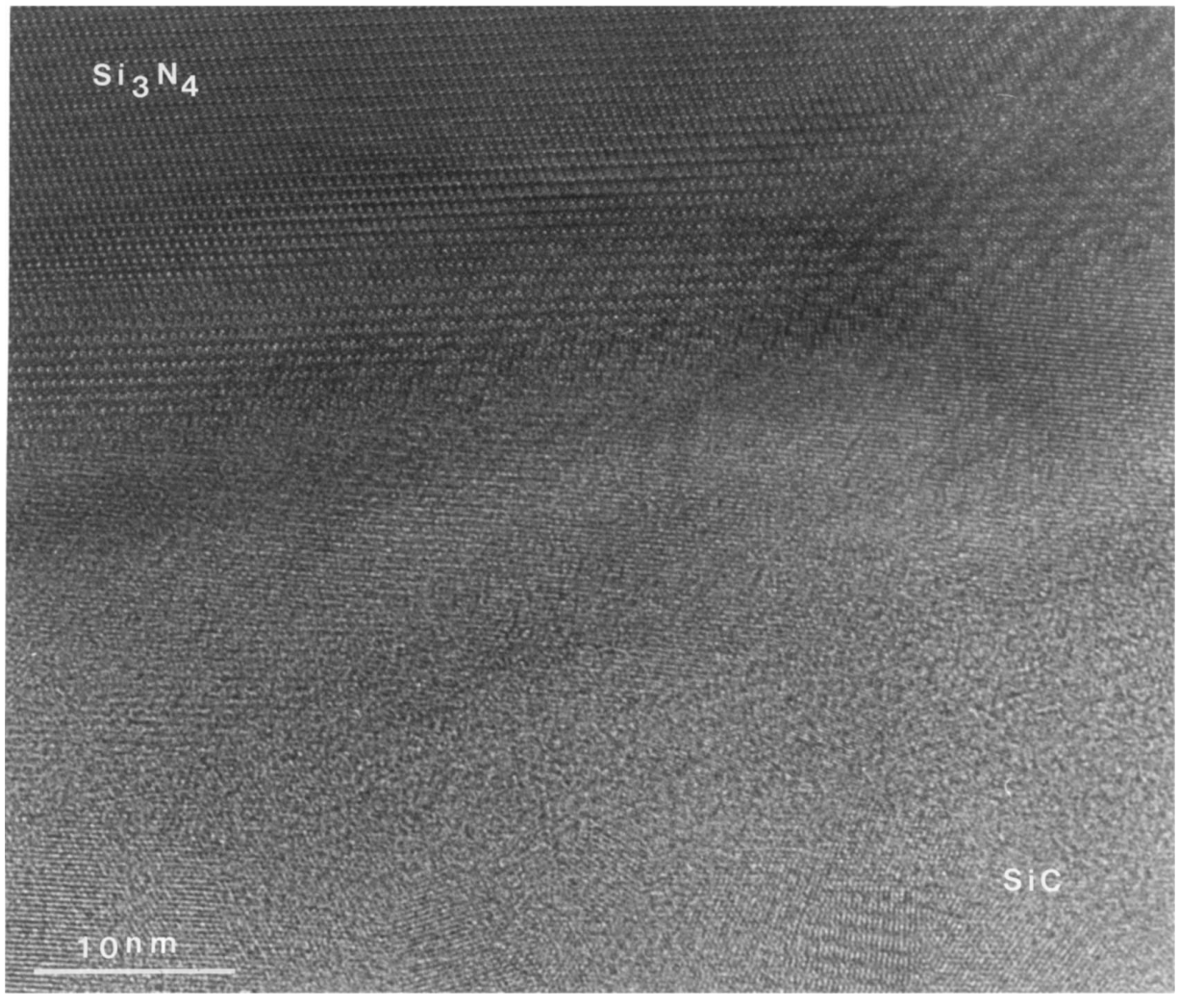

(b)

Figure 11 (a) Bright-field TEM image showing an interfacial region between Hi-Nicalon fiber and Si_3N_4 matrix without clear signs of the presence of the pyrolytic carbon coating and (b) HRTEM image showing direct bonding between SiC of the Hi-Nicalon fiber and a Si_3N_4 grain due to the absence of pyrolytic carbon.

reactor. SiO_2 is a more stable phase than SiC (lower Gibbs-free energy) and therefore may be present as a native oxide on the fiber surface. The different starting conditions for deposition result in reduction of the SiO_2 if the deposition starts at the exit of the reactor, but no reduction if the deposition starts at the entrance of the reactor. The changing gas/vapour composition, e.g. the observed increase in hydrogen concentration

during passage through the reactor due to cracking of the hydro-carbons (propylene), could be responsible for this difference in reduction ability at the entrance or exit of the reactor.

(ii) Oxygen or oxygen containing compounds are introduced as impurities by the gas flow in the reactor and react with the SiC at the fiber surface to form SiO_2 before the C_P is deposited. Alternatively, an oxygen-rich C_P region is deposited first which in a later stage can react with the fiber surface, for example during the hot-pressing at 1550 °C. The difference between starting the deposition either at the entrance or at the exit of the reactor is obvious. The oxygen (compound) reacts directly at the entrance of the reactor and is depleted at the exit. Then, the presence of oxygen during the start of the deposition is harmful but at the end of deposition is harmless.

4.2. Influence of hot-pressing temperature

Similar to sample I, sample III shows brittle behaviour. However, the origin of the brittleness is totally different. In the case of sample type I the pull-out of the fibers during tensile testing is huge and in case of sample type III is short and for a fraction of the fibers absent. For sample I the load transfer from matrix to fiber is insufficient and in contrast for sample III appears to be too strong and direct to be optimal. As was observed for sample III the C_P coating between the matrix and the fibers was often not able to deflect an advancing matrix crack from perpendicular to parallel to the fiber axis.

As stated in the introduction of this chapter sample I and III can not be compared conclusively. On the other hand, for sample II and III only the hot-pressing temperature during manufacturing of the CMCs changed from 1550 to 1600 °C. This change of temperature results in some effects observable in the samples by TEM: (i) porosity observed in the 1550 °C hot-pressed samples becomes unobservable in the 1600 °C samples; (ii) bonding between the C_P coating and the Si_3N_4 matrix is considerably stronger in the case of 1600 °C than in the case of 1550 °C. This difference in bonding can be deduced from the often observed detachment between the matrix and the coating in the case of the 1550 °C samples whereas this detachment is more or less absent in the 1600 °C samples, but is replaced by debonding in the coating itself. Bonding between the coating and the fiber is, for both sample types, invariably strongest.

Concomitant with the decrease in the volume fraction of pores, i.e. also of pores at the matrix coating interface, an increase in bond strength between the Si_3N_4 and the C_P is achieved. At first sight this seems an improvement. However, this is not the case as follows from the pseudo-plastic versus brittle behaviour, as observed by tensile testing, of the 1550 and 1600 °C hot-pressed samples. Apparently, the 200 nm thick C_P coating alone (this is the nominal thickness, but for a major part of the coating is less; cf. Section 3 and below) is not efficient in deflecting an advancing matrix crack and if deflecting may cause brittle break-out of Si_3N_4 particles (cf. Fig. 10b) and hence is not able to give a load transfer from matrix to fiber with a suitable sliding friction. Instead the loading of the fiber becomes too direct and approaches the one of a direct (strong) bonding between the SiC fibers and the Si_3N_4 matrix and becomes similar to the behaviour of a monolithic ceramic. Now, if the (chemical) bonding between the matrix and the coating is sufficient weak, deflection of an advancing matrix crack along the matrix/coating interface is possible. Since this interface is very rough also due to the non-uniform thickness of the coating (cf. Section 3), mechanical bonding will start to operate during pull-out which certainly leads to loading of the coating involving sliding friction. On the other hand the roughness of the fibers is very low and if the chemical bond between the fiber and the coating is weak mechanical bonding will not operate at the fiber/coating interface and an easy pull-out of the fibers results. This is exactly what holds for sample type I.

The bonding between the matrix and the coating at 1600 °C hot-pressing, in conjunction with a (too small) nominal coating thickness of 200 nm, is too strong and hinders deflection of an advancing matrix crack. However, if the coating thickness is increased sufficiently the structure of the pyrolytic carbon coating should be a guarantee for the ability to deflect advancing matrix cracks parallel to the fiber axis before the fiber is reached. This is indeed the case as can be concluded from the excellent pseudo-plastic behaviour of sample types with a nominal coating thickness of 400 nm hot-pressed at 1600 °C [10]. On the other hand, decreasing the nominal thickness of the coating from 200 to 100 nm gives for both the hot-pressing temperatures of 1550 and 1600 °C brittle behaviour [10]. In light of the discussion above this is not obvious, because the sufficient weak bonding between matrix and coating at 1550 °C are not expected to give principal differences between these 2 coating thicknesses.

However, there is another phenomenon involved which has not been taken along in the present discussion. This concerns the observed on average smaller than nominal coating thickness (easily a factor of 2 for the 200 nm coatings), the observation of pyrolytic carbon in-between Si_3N_4 grains at relative large distances from a fiber and in some cases the observed direct bonding between the matrix and the fibers (cf. Figs 5 and 11). Probably, these effects can be attributed predominantly to the manufacturing, the slurry infiltration and the hot-pressing, of the CMCs. The relative decrease of the coating thickness and the probability of direct matrix-fiber bonding are expected to increase for decreasing coating thickness and it is also tentative to expect this for increasing hot-pressing temperature. Comparing samples II and III this expectation seems to be justified and may be also an important factor that contributes to the transition from pseudo-plastic to brittle behaviour on increasing the hot-pressing temperature from 1550 to 1600 °C. However the number of fibers analyzed with the present TEM study is much too small to make a statistical significant statement on this matter. On the other hand, the observed lengths of fiber pull-out at the fracture surface is for a significant fraction of the fibers very small and clearly less for

sample type III than II, whereas the relative spread in pull-out lengths is much larger for sample type III than II. These observations can be regarded as an indication for an increased probability of direct matrix-fiber bonding. Further, the transition from pseudo-plastic to brittle behaviour on decreasing the coating thickness from 200 to 100 nm for a hot-pressing temperature of 1550 °C can also be explained well by this observed decrease in coating thickness and by the increased probability of direct bonding between matrix and fiber.

5. Conclusions

Si_3N_4 matrix composites reinforced with unidirectionally oriented, pyrolytic carbon pre-coated, Hi-Nicalon (SiC) fibers, were studied using tensile testing and transmission electron microscopy. Three types of samples were studied, all having a nominal coating thickness of 200 nm. The composites of type I and II were densified by hot pressing at 1550 °C and type III at 1600 °C. The fibers were coated with pyrolytic carbon using a CVD process in which the direction of the gas flow was opposite to the pulling direction of the fibers through the reactor for samples II and III and both directions were the same for sample I. Tensile testing indicated brittle behaviour with huge pull-out of the fibers for sample I (fracture stress 430 ± 50 MPa), pseudo-plastic behaviour for sample II with a fracture stress of 700 ± 50 MPa and brittle behaviour with little or no pull-out of the fibers for sample III (fracture stress 430 ± 20 MPa).

From the TEM observations it became apparent that in sample I insufficient bonding between the coating and the fiber was achieved. For sample II the coating/matrix interface appeared weakest and for sample III the preferable location for debonding was in the coating itself. The brittleness of sample I is obvious since no significant load transfer from matrix to fiber occurs and the sample behaves like monolithic Si_3N_4. The brittle behaviour of sample III is not obvious, but can be understood from the relative too strong bonding between the matrix and the coating in conjunction with a too small thickness of the coating which results in insufficient deflection of advancing matrix cracks from perpendicular to parallel to the fiber axis. A transition from brittle to pseudo-plastic behaviour occurs by either increasing the coating thickness or, less preferable, decreasing the bond strength between the coating and the matrix. This last step occurs for sample II by the decrease of the hot-pressing temperature from 1600 to 1550 °C. The transition from pseudo-plastic to brittle behaviour is strongly affected by the observed (on average) smaller than nominal coating thickness and the direct bonding between matrix and fiber. A decrease in coating thickness or an increase in hot-pressing temperature, explaining the difference between sample II and III, induces this transition to brittleness.

The significant difference in bond strength between the fiber and the coating as a consequence of the difference in CVD condition is related to the change in composition of the reactants at the entrance and the exit (with respect to gas flow) of the reactor. If deposition starts at the entrance, SiO_2 at the fiber/coating interface is present, whereas SiO_2 is absent if deposition starts at the exit of the reactor. SiO_2 at the fiber/coating interface deteriorates the fiber/coating bond strength.

References

1. E. SABOURET, J. B. VEYRET and E. BULLOCK, in Proc. 2nd Int. Conf. High-Temperature Ceramic-Matrix Composites I, edited by A. G. Evans and R. Naslain (Santa Barbara, 1995) Ceramic Trans. Vol. 57, p. 299; K. NAKANO and A. KAMIYA, in Proc. 5th Europ. Conf. composite Materials (Europ. Assoc. Composite Materials, 1992) p. 697.
2. L. PORTE and A. SARTRE, *J. Mater. Sci.* **24** (1989) 271; M. H. JASKOWIAK and J. A. DICARLO, *ibid.* **72** (1989) 192.
3. C. LABRUGERE, A. GUETTE and R. NASLAIN, *J. Eur. Ceram. Soc.* **17** (1997) 623–640; C. LABRUGERE, L. GUILLAUMAT, A. GUETTE and R. NASLAIN, *ibid.* **17** (1997) 641–657.
4. K. OKAMURA, M. SATO, T. SEGUSHI and S. KAWANISHI, in Proc. 1st Jap. SAMPE Symp., 1989, p. 929; M. TAKEDA, Y. IMAI, H. ICHIKAWA, T. ISHIKAWA, N. KASAI, T. SEGUSHI and K. OKAMURA, *Ceram. Eng. Sci. Proc.* **14** (1993) 540; M. TAKEDA, J. SAKAMOTO, Y. IMAI, H. ICHIKAWA and T. ISHIKAWA, *ibid.* **15** (1994) 133; R. BODET, X. BOURRAT, J. LAMON and R. NASLAIN, *J. Mater. Sci.* **30** (1995) 661; A. R. BUNSELL, M. H. BERGER and N. HOCHET, in Proc. 2nd Int. Conf. High-Temperature Ceramic-Matrix Composites II, edited by A. G. Evans and R. Naslain (Santa Barbara, 1995) Ceramic Trans. Vol. 58, p. 85.
5. J. B. VEYRET, P. TAMBUYSER, C. OLIVIER, E. BULLOCK and M.-H. VIDAL-SETIF, *J. Mater. Sci.* **32** (1997) 3457–3462.
6. K. NAKANO, K. SASAKI, H. SAKA, M. FUJIKURA and H. ICHIKAWA, in Proc. 2nd Int. Conf. High-Temperature Ceramic-Matrix Composites II, edited by A. G. Evans and R. Naslain (Santa Barbara, 1995) Vol. 58, p. 215; A. KAMIYA, K. NAKANO, S. MORIBE, T. IMURA and H. ICHIKAWA, *J. Ceram. Soc. Japan* **102** (1994) 957.
7. C. GRENET, L. PLUNKETT, J. B. VEYRET and E. BULLOCK, in "High-Temperature Ceramic-Matrix Composites II: Manufacturing and Materials Development," Vol. 58, edited by A. G. Evans and R. Naslain (Santa-Barbara, CA, 1995) p. 125.
8. P. BERTRAND, M. H. VIDAL-SETIF and R. MEVREL, *J. Physique IV* **C5** (1995) 769–776.
9. M. H. VIDAL-SETIF and J. L. GERARD, *ibid.* **C2** (1991) 681–688.
10. C. OLIVIER, J. B. VEYRET and M. H. VIDAL-SETIF, *Key Engineering Materials* **127–131** (1997) 753.
11. P. FOURVEL, P. SYLVESTRINI, M. H. ROUILLON, J. VINCENS and M. GOMINA, *J. Mater. Sci.* **25** (1990) 5163.
12. I. BARIN and O. KNACKE, "Thermochemical Properties of Inorganic Substances" (Springer-Verlag, Berlin, 1973).

Received 30 July 1998
and accepted 9 March 1999